



Article

Immobilization of Lipase A from *Candida antarctica* onto Chitosan-Coated Magnetic Nanoparticles

Rodolpho R. C. Monteiro ¹, Paula J. M. Lima ¹, Bruna B. Pinheiro ¹, Tiago M. Freire ², Lillian M. U. Dutra ², Pierre B. A. Fechine ², Luciana R. B. Gonçalves ¹, Maria C. M. de Souza ³, José C. S. dos Santos ^{3,*} and Roberto Fernandez-Lafuente ^{4,*}

¹ Departamento de Engenharia Química, Universidade Federal do Ceará, Campus do Pici, Bloco 709, Fortaleza 60455760, CE, Brazil

² Departamento de Química Analítica e Físico-Química, Universidade Federal do Ceará, Campus do Pici, Bloco 940, Fortaleza CEP 60455760, CE, Brazil

³ Instituto de Engenharias e Desenvolvimento Sustentável, Universidade da Integração Internacional da Lusofonia Afro-Brasileira, Campus das Auroras, Redenção 62790970, CE, Brazil

⁴ Departamento de Biotecnología, ICP-CSIC, Campus UAM-CSIC, 28049 Madrid, Spain

* Correspondence: jcs@unilab.edu.br (J.C.S.d.S.); rfl@icp.csic.es (R.F.-L.)

Received: 12 July 2019; Accepted: 15 August 2019; Published: 17 August 2019



Abstract: In this communication, lipase A from *Candida antarctica* (CALA) was immobilized by covalent bonding on magnetic nanoparticles coated with chitosan and activated with glutaraldehyde, labelled CALA-MNP, (immobilization parameters: 84.1% ± 1.0 for immobilization yield and 208.0 ± 3.0 U/g ± 1.1 for derivative activity). CALA-MNP biocatalyst was characterized by X-ray Powder Diffraction (XRPD), Fourier Transform Infrared (FTIR) spectroscopy, Thermogravimetry (TG) and Scanning Electron Microscope (SEM), proving the incorporation of magnetite and the immobilization of CALA in the chitosan matrix. Besides, the immobilized biocatalyst showed a half-life 8–11 times higher than that of the soluble enzyme at pH 5–9. CALA showed the highest activity at pH 7, while CALA-MNP presented the highest activity at pH 10. The immobilized enzyme was more active than the free enzyme at all studied pH values, except pH 7.

Keywords: lipase A from *Candida antarctica*; chitosan; magnetic nanoparticles; characterization

1. Introduction

Chemical and enzymatic catalysts are both effective for industrial applications [1,2]; nevertheless, chemical catalysis possesses several drawbacks, such as high energy consumption, undesirable by-product formation and equipment corrosion [3,4]. Enzymatic catalysis, on the other hand, is not as energy-demanding due to the mild operating conditions. It is also selective and specific, preventing undesired modifications of substrate and formation of toxic by-products, and it also presents very low environmental impact [5–9].

Lipases (triacylglycerol acyl hydrolases, E.C. 3.1.1.3–IUPAC) belong to a group of enzymes whose physiological function is to catalyze the hydrolysis of oils and fats [10]; apart from hydrolysis, under micro-aqueous environment, they are able to catalyze reactions such as esterification, transesterification, alcoholysis, acidolysis, epoxidations, etc., [11–15]. Basidiomycetous yeast *Candida antarctica* produces two different types of lipases, lipase A (CALA) and lipase B (CALB) [16]. CALB is the most extensively studied lipase in chemistry and fine chemistry [17], food technology [18] and bioenergy [19]; its crystalline structure was first reported in 1994 [20], whereas CALA had its crystalline structure more recently reported [21]. CALA has some useful properties to catalyze reactions, including high thermostability and the ability to tolerate a wide range of pHs [22,23].

The use of enzymes in their free or soluble forms evidences some problems related to low operational stability, difficult recovery and subsequent reuse of these biocatalysts [24]. However, such problems can be overcome when appropriate immobilization techniques are employed [25]; furthermore, once immobilized, enzymes exhibit greater resistance to pH, thermal and storage variations [26–31].

Depletion of oil reserves and an increase in crude oil prices coupled with the demand to protect the environment against pollution caused by mineral lubricating derived from petroleum and its uncontrolled disposal have driven to a growing interest in the use of biolubricants [32–34]. Biolubricants are an alternative to traditional lubricants, since they have valuable physicochemical properties (high lubricity, high viscosity index, high flash point and low vapor pressure, for example); besides having biodegradability and low toxicity towards humans and Nature [35,36]. Biolubricants may be produced from various vegetable oils, and it is also possible to produce them from synthetic esters and oils of fossil origin that meet biodegradability and toxicity criteria [37,38].

Literature reports a wide application of vegetable oils in bioenergetic industry; however, comparatively, there are few studies on the use of vegetable oils for lubrication purposes. Most vegetable oils used for these latter purposes are part of the human food chain (e.g., sunflower, soybean, corn, palm and coconut), which makes them unsuitable in the long run [39–42]. Thus, it is necessary to turn towards alternative sources of raw materials to produce biolubricants, preferably based on non-edible oils. An underutilized feedstock for biolubricant production is tilapia oil (*Oreochromis niloticus*) [43], which is one of the most widely cultivated fish in the world. In Brazil, tilapia accounts for approximately 45.4% of freshwater aquaculture production. There are large amounts of fish waste, especially viscera, which correspond to 7.5 to 15% of the weight of the fish [44,45]. Most of the time, residues from fish farming activity are dumped in landfills or directly into bodies of water, causing environmental problems. In this sense, the use of these residues to produce biolubricants will thus cover two environmental issues: production of non-toxic lubricants and use of a contaminating residue [46,47]. One point that makes interesting this material in the context of the paper, is that biolubricants use to give high viscosity and makes the recovery of immobilized biocatalysts difficult.

In this context, association of enzymes with magnetic nanoparticles (MNPs) may allow an easy separation of the enzymatic biocatalyst from the reaction medium by exposure to an external magnetic field, enabling a subsequent reuse of the biocatalyst [48]. The employed iron magnetic nanoparticles are solid dispersion particulates that exhibit paramagnetic properties at typical sizes of 10 to 20 nm [49]. The use of MNPs as solid supports for enzymatic immobilization has attracted considerable interest in the last decades; furthermore, low porosity and high mechanical and thermal stability are important properties of these nanostructured magnetic supports [50–52].

These naked iron nanostructures tend to aggregate and to become oxidized. This produces the loss of paramagnetism and dispersibility [53]. To overcome such problems, aiming at enzymatic immobilization, the surface of this type of solid support has been functionalized with organic polymers, silica or metalorganic structures [54]. Among these materials, we would like to remark chitosan, an abundant biopolymer with good biocompatibility and low toxicity. Chitosan is a copolymer obtained from the deacetylation of chitin, being a weak base, water insoluble in neutral or basic medium or in organic solvents, but it is soluble in dilute acidic media (pH < 6.5) [55,56]. Chitosan has been used in a wide variety of industrial fields such as biomedicine [57], papermaking [58], wastewater treatment [59], agriculture [60] or enzyme immobilization [61,62], among others.

For enzyme immobilization, chitosan has been used as a functional material since it offers a unique set of characteristics: biocompatibility, biodegradability to harmless products, nontoxicity, physiological inertness, antibacterial properties, heavy metal ions chelation, gel forming properties and hydrophilicity [61]. As coating for iron MNPs, chitosan controls size distribution, and thus enables the colloidal stability of these nanostructures [39,63–65] It also adds some new groups to the surface of the nano particles, introducing primary amino and hydroxyl groups.

Enzymes can be attached on the support by physical or chemical bonds [66]. Glutaraldehyde is generally used as the activating agent to covalently immobilize enzymes, especially on aminated supports [67], due to its high versatility [68,69]. When it is used, glutaraldehyde reacts with primary amino groups of the enzyme and the support; thus, a heterofunctional support is generated, having both physical and chemical interaction capacities [70,71].

The main objective of this communication is to evaluate the immobilization of lipase A from *Candida antarctica* on chitosan-coated magnetic nanoparticles activated with glutaraldehyde, here named CALA-MNP. Finally, we will check the feasibility of recovering the enzyme after producing biolubricants using tilapia fish viscera oil as source of the fatty acids.

2. Results and Discussion

2.1. Immobilization Parameters

The immobilization parameters were evaluated after 3 hours of immobilization, employing a protein load of 1 mg of protein per g of support for the hydrolysis of *p*-NPB (0.5 mM). The reference enzyme solutions (an enzyme prepared under identical conditions to the free enzyme but in absence of support) maintained full activity during all immobilization process. That way, immobilization yield could be calculated by the decrease of activity in the supernatant. For the covalent immobilization ($\text{Fe}_3\text{O}_4\text{@CHI-GLU-CALA}$), the immobilization yield was around 84, the theoretical activity was just over 200 U/g, the actual derivative activity was under 70. This gave an expressed activity of more than 95%, as it can be seen in Table 1, which also presents the immobilization parameters for the biocatalyst prepared using no glutaraldehyde activated particles ($\text{Fe}_3\text{O}_4\text{@CHI-CALA}$). The enzyme immobilized on glutaraldehyde activated nanoparticles performed better than the non-activated nanoparticles, showing that glutaraldehyde plays a significant role on enzyme immobilization.

Table 1. Immobilization parameters of $\text{Fe}_3\text{O}_4\text{@CHI-GLU-CALA}$ and $\text{Fe}_3\text{O}_4\text{@CHI-CALA}$: Immobilization yield (IY), theoretical activity (At_T), actual biocatalyst activity (At_D) and recovered activity (At_R).

Biocatalyst	IY(%)	At_T (U/g)	At_D (U/g)	At_R (%)
$\text{Fe}_3\text{O}_4\text{@CHI-GLU-CALA}$	84.1 ± 1.0	212.2 ± 1.0	208.0 ± 3.0	98.0 ± 3.0
$\text{Fe}_3\text{O}_4\text{@CHI-CALA}$	44.3 ± 1.5	123.1 ± 1.5	120.8 ± 2.0	98.1 ± 2.0

Osuna et al. immobilized lipase from *Aspergillus niger* on magnetic nanoparticles coated with chitosan and activated with glutaraldehyde, achieving an immobilization yield of $90.1 \pm 1.1\%$ and a mass activity of 309.5 ± 2.0 U/g [72]; Santos et al. obtained an immobilization yield of $94.70 \pm 1.37\%$ for the immobilization of CALB on chitosan support activated with glutaraldehyde [25]. Therefore, the immobilization parameters obtained in this study are in agreement with those reported in the literature, especially for the immobilization yield.

Glutaraldehyde, under the conditions used, is able to modify all the amino groups of chitosan, which can react with the amino residues of the lipase [72,73]. Therefore, lipase can be covalently immobilized on magnetic nanoparticles coated with chitosan and activated with glutaraldehyde base linkage between the aldehyde group of glutaraldehyde and the terminal amino group of lipase.

Pinheiro et al. immobilized lipase B from *Candida antarctica* on chitosan beads, achieving an immobilization yield of $55.6 \pm 1\%$ and $91.0 \pm 1\%$ when glutaraldehyde was used as activating agent [62]. Similarly, in this communication, the support presented a better performance for immobilization when activated with glutaraldehyde, even though the results clearly show that the support is able to immobilize CALA via ionic exchange. The modification of chitosan also reduces water retention capacity and makes it more resistant, improving its performance [74].

2.2. Effect of pH on the Thermal Stability of CALA Biocatalysts

At 85 °C, CALA and CALA-NPM were evaluated for thermal and pH inactivation. The stability of CALA-NPM was the highest at pH 9 ($t_{1/2}$ = 222 min) followed by that at pH 5 ($t_{1/2}$ = 92 min) and at pH 7 ($t_{1/2}$ = 62 min). Free CALA also presented the highest stability at pH 9 ($t_{1/2}$ = 27 min), followed by pH 5 ($t_{1/2}$ = 10.1 min) and pH 7 ($t_{1/2}$ = 5.7), but with significantly lower performance compared to the immobilized enzyme, as it can be seen in Table 2.

Table 2. Half-life for CALA and CALA-MNP at 85 °C and pHs 5, 6 and 9.

Biocatalyst	Half-Life ($t_{1/2}$, min)		
	pH 5	pH 7	pH 9
CALA	10.1	5.7	27
CALA-MNP	92	62	222

CALA is quite stable over a relatively broad pH range (6–9) [75], being highly stable in its immobilized form and it can be used at elevated temperature for thousands of hours without any significant loss in activity [76]. At pH 7, both CALA and CALA-MNP presented the lowest half-lives (5.7 and 62 min, respectively). This may be caused by the use of sodium phosphate at pH 7, as recently reported, it has negative effects on lipase stability [77].

In this case, stabilization due to immobilization ranged from 8.2 to 10.8. The lower the enzyme stability, the higher the stabilization due to immobilization.

2.3. Effect of pH on CALA Biocatalysts Activity

In order to evaluate the effect of pH on the biocatalysts performance, their activity was evaluated from pH 5 to pH 10, which are the limits of the substrate stability. As it can be seen in Figure 1, the soluble enzyme presented a quite flat profile, with a maximum at pH 7 and a lower activity at more acid or basic pH values. Other authors studied the effect of pH on the activity of CALA and observed the same profile obtained in this study, the highest activity was obtained at pH 7 [23,75,78].

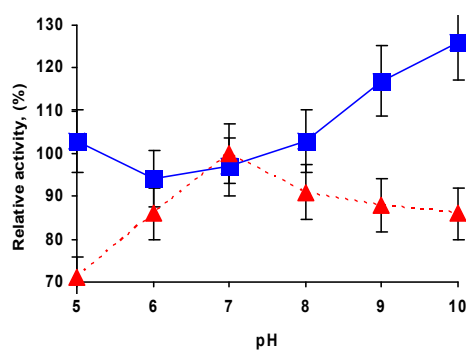


Figure 1. Effect of the pH value on *p*-NPB activity of CALA (red triangles) and CALA-MNP (blue squares). Further details are given in Section 3. 100% is considered the activity of the free enzyme at pH 7 (optimal conditions for the enzyme), and correspond to around 210 U/mg.

For the immobilized enzyme, the effect of pH on the biocatalyst activity was fully different. In that case, a minimum activity at pH 6 was observed. Thus, although at pH 7 both immobilized and free enzymes have almost the same activity, under all the other pH values the immobilization of the enzyme increased significantly the specific activity of the enzyme (by a 50% at pH 9 or 10). Without discarding changes in the ionic interactions of the enzyme with the support that will depend on the pH value [79], this can be due to the increase in enzyme stability and/or conformational changes caused during immobilization.

2.4. Characterization of the Nanoparticles and Biocatalysts

In order to verify the incorporation of magnetite and the immobilization of CALA in the CALA-NPM, Fourier Transform Infrared (FTIR) spectroscopy absorption spectra were measured for the samples: Fe_3O_4 , CHI, $\text{Fe}_3\text{O}_4@CHI$, $\text{Fe}_3\text{O}_4@CHI\text{-GLU}$ and $\text{Fe}_3\text{O}_4@CHI\text{-GLU}\text{-CALA}$ (Figure 2a). The crystalline structure present in the systems was determined by X-ray Powder Diffraction (XRPD). Figure 2b showed the profile diffraction peaks obtained for $\text{Fe}_3\text{O}_4@CHI$ and $\text{Fe}_3\text{O}_4@CHI\text{-GLU}\text{-CALA}$. Thermogravimetry (TG) was used to evaluate the thermal stability and to quantify the relative organic amount in the nanocomposites (Figure 2c,d).

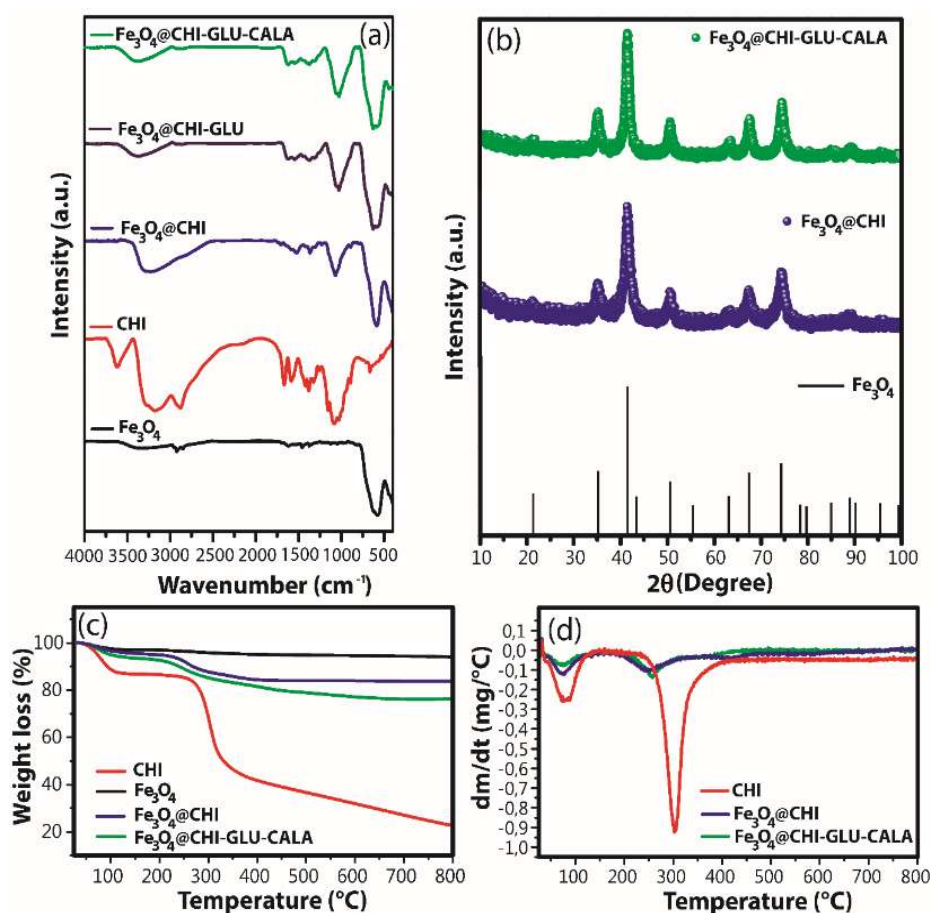


Figure 2. (a) FTIR, (b) XRPD, (c,d) TG and DTG of the synthesized samples.

For the FTIR analysis, for Fe_3O_4 , $\text{Fe}_3\text{O}_4@CHI$ and $\text{Fe}_3\text{O}_4@CHI\text{-GLU}\text{-CALA}$ samples, bands around 590 and 3340 cm^{-1} were respectively assigned to Fe–O deformation and O–H stretching vibration of water adsorbed on the magnetite surface [80]. A strong band around 590 cm^{-1} was not observed in CHI spectrum. Thus, this band can be used to confirm the presence of magnetite in the composites. In CHI, $\text{Fe}_3\text{O}_4@CHI$ and $\text{Fe}_3\text{O}_4@CHI\text{-GLU}$ spectra, C–O stretching vibration of glycosidic bonds was observed around 1075 cm^{-1} [81]. For CHI spectrum, the bands at 1319 , 1379 and 1421 cm^{-1} can be referred to C–N stretching of amino groups and bending vibration of methylene and methyl groups, respectively [82,83]. For CHI and $\text{Fe}_3\text{O}_4@CHI$ samples, the absorption around 1580 cm^{-1} is characteristic of -NH_2 bending vibration [83]. This band was not observed in $\text{Fe}_3\text{O}_4@CHI\text{-GLU}$ spectrum, suggesting that the crosslinking reaction between CHI and glutaraldehyde occurred. Additionally, the $\text{Fe}_3\text{O}_4@CHI\text{-GLU}$ spectrum presents an absorption at 1622 cm^{-1} that can be assigned to C=O stretching vibration of amide groups and C=N of imine groups [64]. Interestingly, the spectra of $\text{Fe}_3\text{O}_4@CHI\text{-GLU}$ and $\text{Fe}_3\text{O}_4@CHI\text{-GLU}\text{-CALA}$ are very similar. However, the relative

intensity of the band at 1622 cm^{-1} is greater in $\text{Fe}_3\text{O}_4\text{@CHI-GLU-CALA}$, suggesting an increase in the density of imine groups in its structure due to the crosslink reaction between CHI and CALA.

For XDR analysis, for $\text{Fe}_3\text{O}_4\text{@CHI}$ and $\text{Fe}_3\text{O}_4\text{@CHI-GLU-CALA}$ samples, peaks were identified at 21.3° , 35.3° , 41.3° , 50.7° , $63.^\circ$ and 67.5° which can be assigned to (111), (220), (311), (400), (422) and (511) planes of Fe_3O_4 cubic spinel (ICSD, file-01-086-1340). Thus, it is important to note that the strategy used to synthesize nanocomposites was efficient, once the CHI coating can act as a protecting agent against magnetite oxidation and as site for lipase immobilization.

For TG analysis, in Figure 2c, the first thermal event, related to residual water loss, occurs between 30 and $125\text{ }^\circ\text{C}$ for all samples [62]. For this event, the losses of 2.90%, 12.88%, 3.03% and 5.95% were observed for Fe_3O_4 , CHI, $\text{Fe}_3\text{O}_4\text{@CHI}$ and $\text{Fe}_3\text{O}_4\text{@CHI-GLU-CALA}$, respectively. In addition, DTG shows that the rate of degradation for this first thermal event increases following the order $\text{Fe}_3\text{O}_4\text{@CHI-GLU-CALA}$, $\text{Fe}_3\text{O}_4\text{@CHI}$ and CHI. This can be assigned to the occupation of the hydrophilic sites of CHI, since the amine and hydroxyl groups must interact with the surface of magnetite and CALA, becoming less available to interact with water molecules [84]. The main polymeric degradation occurs in the temperature range of 200 to $414\text{ }^\circ\text{C}$ for CHI and 180 to $493\text{ }^\circ\text{C}$ for $\text{Fe}_3\text{O}_4\text{@CHI}$ and $\text{Fe}_3\text{O}_4\text{@CHI-GLU-CALA}$ [85]. The decrease of the polysaccharide thermal stability may be assigned to the breakdown of CHI-CHI intermolecular interaction, since the amine and hydroxyl groups of CHI, besides interacting with Fe_3O_4 , participate of crosslinking reactions with the enzyme [86]. In DTG curves, the decrease in thermal stability is evident for CHI, since the maximum rate of the weight loss occurred at 302, 257 and $250\text{ }^\circ\text{C}$ for CHI, $\text{Fe}_3\text{O}_4\text{@CHI-GLU-CALA}$ and $\text{Fe}_3\text{O}_4\text{@CHI}$ samples. Additionally, the weight loss for the second thermal event was 49.77, 11.17 and 14.10% for CHI, $\text{Fe}_3\text{O}_4\text{@CHI}$, and $\text{Fe}_3\text{O}_4\text{@CHI-GLU-CALA}$ samples, respectively. For all the samples, the thermal degradation continues even in smaller proportion until $800\text{ }^\circ\text{C}$, corresponding to the maximum weight loss of 6.03, 77.33, 16.21 and 23.62% for Fe_3O_4 , CHI, $\text{Fe}_3\text{O}_4\text{@CHI}$ and $\text{Fe}_3\text{O}_4\text{@CHI-GLU-CALA}$ samples, respectively. Since the sample $\text{Fe}_3\text{O}_4\text{@CHI-GLU-CALA}$ presents a maximum weight loss greater than $\text{Fe}_3\text{O}_4\text{@CHI}$, it can be inferred that CALA was successfully incorporated on the CHI surface.

Scanning electron microscope (SEM) images of CHI, $\text{Fe}_3\text{O}_4\text{@CHI}$ and $\text{Fe}_3\text{O}_4\text{@CHI-GLU-CALA}$ are shown as inset Figure 3a,c,d. SEM images of CHI, $\text{Fe}_3\text{O}_4\text{@CHI}$ and $\text{Fe}_3\text{O}_4\text{@CHI-GLU-CALA}$ are shown as inset Figure 3a,c,d. These images illustrate the change that occurs on the CHI surface after the process of modification with Fe_3O_4 . It was seen that CHI has a morphology similar to crushed shells (Figure 3a), with low roughness and porosity. After the incorporation of Fe_3O_4 in CHI matrix, the micrographs showed a huge change on the roughness, since the surface presents agglomerates that can be assigned to $\text{Fe}_3\text{O}_4\text{@CHI}$ nanocomposite (Figure 3c).

No significant changes were observed on the nanocomposite surface after CALA immobilization (Figure 3e, inset). In order to evaluate the composition of the samples surface, EDS maps and EDS spectra were carried out (Figure 3a–f). From the EDS spectra, it was possible to obtain the weight percentage of the element on the surface of the nanocomposites. Figures 3d and 4e showed that the surface of $\text{Fe}_3\text{O}_4\text{@CHI}$ and $\text{Fe}_3\text{O}_4\text{@CHI-GLU-CALA}$ samples is rich in iron with high homogeneity. For the CHI sample, no iron was observed in the EDS spectra (Figure 3b). Additionally, the percentage of carbon is higher in $\text{Fe}_3\text{O}_4\text{@CHI-GLU-CALA}$ than $\text{Fe}_3\text{O}_4\text{@CHI}$. Thus, the EDS spectra suggesting that the CALA immobilization was successful, since the Iron/Carbon ratio decreased.

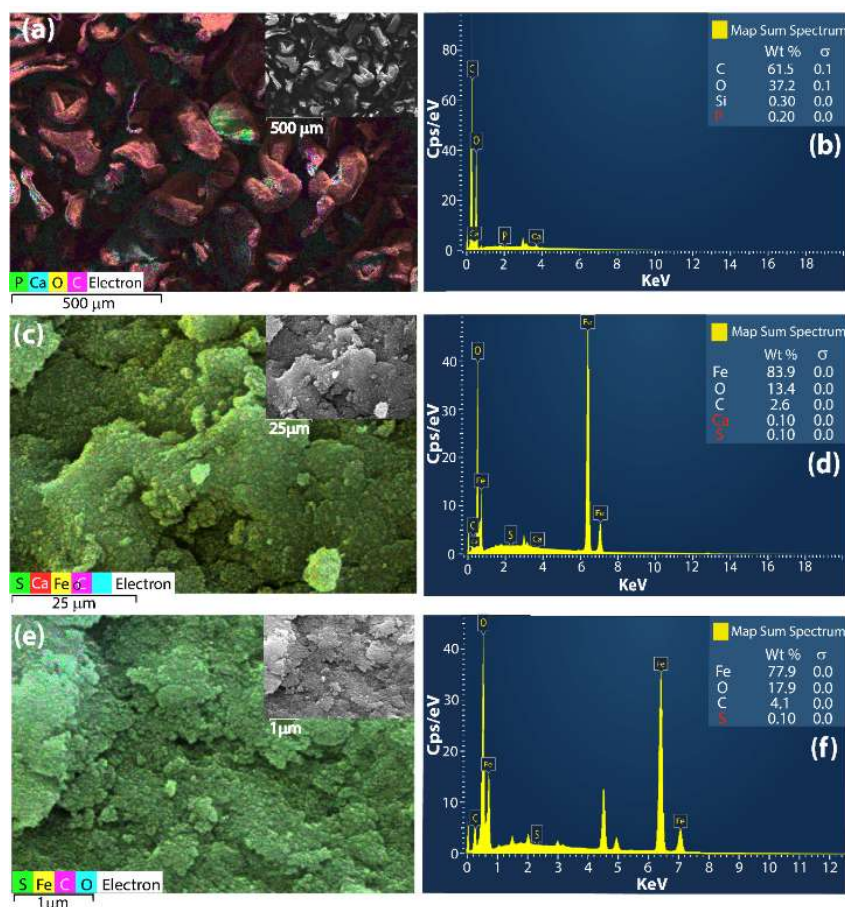


Figure 3. EDS maps, SEM images (inset) and EDS spectra of CHI (a,b), Fe₃O₄@CHI (c,d) and Fe₃O₄@CHI-GLU-CALA (e,f).

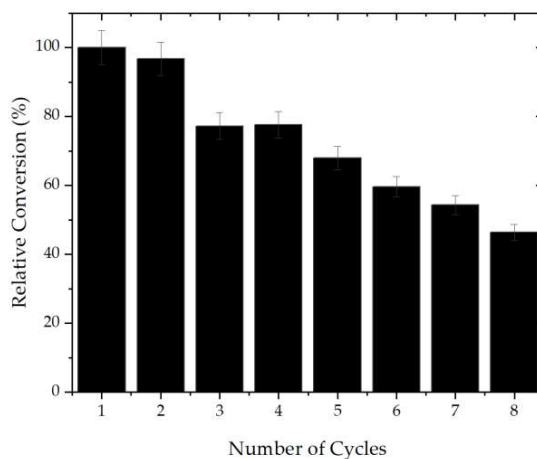


Figure 4. Operational Stability. Reaction medium: CALA-MNP = 208.0 ± 3.0 U/g, 2-ethyl-1-hexanol and free fatty acids from Tilapia oil (1:1) and 2% of content of biocatalyst. The reactions were performed for 24 hours at 30 °C at 200 rpm. Further details are given in Section 3.

2.5. Operational Stability

Enzymes have higher prices than chemical catalysts; thus, to be competitive, immobilized enzymes should be able to be reused several times, maintaining thermal and operational stability [87]. Enzymes are very sensitive to changes in the environment; thus, several cycles of reactions may denature the protein [49], although its immobilization of enzymes promotes its rigidification, which keeps it

active for longer periods of time, allowing consecutive reuse [88]. Using magnetic nanoparticles, and additional problem may be when recovering the biocatalysts in viscous solutions, like when a biolubricant is produced. Thus, we utilized the new biocatalysts in the production of biolubricants using 2-ethyl-1-hexanol and free fatty acids from Tilapia oil (1:1). These conditions permitted to get just around 25% conversion yield, but may be valid to check the possibility of the biocatalyst reuse. Prior to each cycle, the biocatalyst was separated from the reaction medium by magnetization and washed three times with hexane to remove unreacted substrates. As it is shown in Figure 4, for the production of the biolubricant ester, the biocatalyst gave half of the initial conversion after 7 cycles of esterification. This was obtained even with so viscous reaction medium.

3. Materials and Methods

3.1. Materials

The commercial extract of lipase A from *Candida antarctica* (CALA) (20.88 mg/mL) was obtained from Novozymes (Alcobendas, Spain). Iron (III) chloride hexahydrate, iron (II) sulfate heptahydrate, chitosan (50–190 kDa and 75–85% deacetylation degree), 25% (*v/v*) aqueous solution of glutaraldehyde, *p*-nitrophenyl butyrate (*p*-NPB), Triton X-100, 2-ethyl-1-hexanol (99.9%) were supplied by Sigma-Aldrich (St Louis, MI, USA); ammonium hydroxide (28–30%) was supplied by Dinâmica (São Paulo, Brazil). All other reagents and solvents used are of analytical grade. For the elaboration of the experimental design by the Taguchi method, Statistica[®] 10 software (Statsoft, TULSA, OK, USA) was used and, for the creation of the graphics, OriginPro[®] 2017 (OriginLab, Northampton, MA, USA) was used.

3.2. Methods

All experiments were performed at least in duplicate and the results are presented as the average of these values with the standard deviation.

3.2.1. Synthesis of Iron Magnetic Nanoparticles (Fe₃O₄) Functionalized with Chitosan (CHI)

Iron magnetic nanoparticles (Fe₃O₄) functionalized with chitosan (CHI), (labelled Fe₃O₄@CHI in this study) were synthesized by the ultrasonic irradiation assisted by co-precipitation method. Briefly, 50 mg of CHI was suspended in 15 mL of an acetic acid (1%, *v/v*) solution. The resulting mixture was left under moderate stirring at 50 °C for 10 minutes. During this period, 10 mL of iron solution (0.33 M, FeCl₃·6H₂O/FeSO₄·7H₂O, following the molar ratio 2Fe³⁺:Fe²⁺) was added to the solution containing CHI. The final solution was homogenized by using an ultrasound probe with configuration of 20 s on, 10 s off and 50% amplitude. The solution was left for 4 min and then, still under ultrasound irradiation, 2 mL of NH₄OH was slowly added and the system was kept under sonication for more 4 min. Once this was done, the precipitate was separated from the solution by magnetic decantation, washed several times with sodium phosphate buffer solution (25 mM and pH 7.0) to pH 7.0, and then dried and stored in a desiccator under vacuum [64].

3.2.2. Activation of Fe₃O₄@CHI with Glutaraldehyde (GLU)

The amino terminal groups of Fe₃O₄@CHI were activated with glutaraldehyde (Fe₃O₄@CHI-GLU) to promote covalent bonding between the enzyme and the support. To do so, the protocol described by Xie et al., (2009) [89] was utilized, with some modifications. A volume of 25 µL of 25% (*v/v*) glutaraldehyde solution was placed in direct contact with 10 mg of previously dried Fe₃O₄@CHI. The mixture was kept under constant stirring for 2 h at 25 °C and was washed 3 times with 1 mL of 25 mM sodium phosphate at pH 7.0 to remove the excess of glutaraldehyde [89].

3.2.3. Covalent Immobilization of CALA on Fe₃O₄@CHI-GLU

CALA (protein concentration 20.88 mg/mL in the commercial preparation) was immobilized on Fe₃O₄@CHI-GLU, the biocatalyst was named CALA-MNP. To do so, 100 mg of Fe₃O₄@CHI-GLU were suspended in 10 mL of 25 mM sodium phosphate buffer solution at pH 7.0 containing CALA (enzyme loading: 1 mg/g of support) in the presence of 0.01% Triton X-100. The system was kept under constant stirring for 3 h at 25 °C. An identical enzyme solution was prepared in absence of support, as a reference. In our experiments, the activity of this reference was maintained intact during the immobilization time. Finally, the immobilized lipase was separated from the solution by magnetic decantation and washed with 25 mM sodium phosphate buffer solution at pH 7.0 to neutrality. The amount of enzyme immobilized on the support was determined by measuring the initial and final activity of CALA in the supernatant of the immobilization suspension [90].

3.2.4. Immobilization of CALA on Fe₃O₄@CHI

CALA was immobilized on Fe₃O₄@CHI (labelled Fe₃O₄@CHI-CALA in this study) by ionic exchange. A mass of 100 mg of Fe₃O₄@CHI-GLU was suspended in 10 mL of 25 mM sodium at pH 7.0 containing CALA (enzyme loading: 1 mg/g of support) in the presence of 0.01% Triton X-100. The immobilization process was similar to that described in the previous section.

3.2.5. Determination of Enzymatic Activity and Protein Concentration

The activity of the soluble and immobilized enzyme was determined by the hydrolysis of *p*-nitrophenyl butyrate (*p*-NPB) as substrate; the released *p*-nitrophenol concentration was quantified spectrophotometrically at 348 nm. Activity measurements were performed in 25 mM sodium phosphate buffer solution at pH 7.0 and 25 °C, in the hydrolysis of 0.5 mM *p*-NPB (isosbestic point, $\epsilon = 5.236 \text{ mol}^{-1} \cdot \text{cm}^{-1}$). [91]. To initiate the reaction, 50 μL of suspended lipase solution was added to 50 μL of *p*-NPB and 2.5 mL of the buffer solution. An international unit of activity (U) was defined as the amount of enzyme that hydrolyzes 1 μmol of *p*-NPB per minute under the conditions described above. The protein concentration was measured by the Bradford method [92] and bovine serum albumin was used as reference.

3.2.6. Immobilization Parameters

The performance of the immobilized enzyme was evaluated by the immobilization parameters described by Silva et al. [56]. In short, the immobilization yield (IY) was defined as the ratio between the activity of enzymes retained on the support (initial activity – final activity) and initial activity (this is valid if the activity of the reference is maintained during the immobilization time). The theoretical activity (A_{T}) was calculated using the immobilization yield (IY) and the enzyme load (it is the expected activity considering the activity of the free enzyme that has been immobilized). The recovered or expressed activity (A_{R}) was defined as the ratio between the biocatalyst activity (A_{D}) and the theoretical activity (A_{T}).

3.2.7. Thermal and pH Inactivation

The biocatalyst was incubated in sodium acetate buffer (25 mM; pH 5.0), sodium phosphate buffer (25 mM; pH 7.0) or sodium carbonate buffer (25 mM; pH 9.0) at 85 °C. The activity was measured periodically using *p*-NPB and the residual activity was expressed as percentage of initial activity (hydrolytic activity before thermal incubation).

3.2.8. Effect of pH on Biocatalyst Activity

The effect of pH on biocatalyst activity was evaluated; to do so, the biocatalysts were resuspended in 10 mL of sodium phosphate buffer (25 mM; pH 7.0). The activity was measured using *p*-NPB as described previously but using 25 mM buffers at pH varying from 5 to 10 (sodium acetate, sodium

phosphate, and sodium carbonate). The activity was measured when the enzyme was added to the buffer and 15 min after. To ensure internal pH equilibration, the biocatalysts were incubated for 5 min in the measuring buffer before adding *p*-NPB [23].

3.2.9. X-ray Powder Diffraction (XRPD)

XRPD analyses were carried out to confirm the crystalline structures in the samples. The analysis was carried out by X-ray powder diffractometer Xpert Pro MPD (Panalytical, Westborough, MA, USA) using Bragg–Brentano geometry in the range of 10°–100° with a rate of 1° min⁻¹. CoK α radiation ($k = 1.78896 \text{ \AA}$) and the tube operated at 40 kV and 30 mA.

3.2.10. Fourier Transform Infrared (FTIR) Spectroscopy

FTIR analyses were performed in a Perkin Elmer 2000 spectrophotometer used to record between 4000–400 cm⁻¹. Previously, the samples were dried and pressed with KBr (~10 mg of sample to 100 mg of KBr) in disk format.

3.2.11. Thermogravimetry (TG)

TGA were performed with 5 mg of nanoparticles under nitrogen atmosphere using a Thermogravimetric Analyzer Q50 V20. The loss of mass was monitored heating up samples from 25 to 800 °C in a rate of 10 °C min⁻¹.

3.2.12. Scanning Electron Microscope (SEM)

SEM images were performed on a SEM FEG Quanta 450 with EDS. Previously, the samples were deposited on a carbon tape and metalized with silver by the Metalizator Quorum QT150ES. 10 Pa of pressure was applied in the SEM chamber, with an incident electron beam of 20 kV.

3.2.13. Extraction and Purification of Tilapia Oil

The extraction and purification of tilapia oil were performed according to methodology reported by Valle et al. (2013) [43]. In short, 1000 g of viscera of tilapia fish were placed under agitation at 900 rpm and heated at 80 °C for 40 min. Then, the mixture was filtered and decanted overnight. The upper phase (crude oil) was degummed with heated water (5% by weight) and, after centrifugation, the impurities were removed. It was necessary to perform neutralization of tilapia oil due to its high content of free fatty acids (7.2 mg KOH/g). To do so, 500 g of oil were placed under agitation at 250 rpm and heated to 60 °C and then an alkaline solution (4 g of potassium hydroxide and heated glycerin, 10% wt.) was added to the oil, the reaction was carried out for 15 min. After neutralization, the oil was centrifuged, washed with heated water (80 °C), dehumidified at 105 °C for 30 min, vacuum filtered with anhydrous sodium sulfate and stored at ambient temperature. The upper phase, rich in monounsaturated fatty acids, was used for the synthesis of biolubricant esters [43].

3.2.14. Production of Free Fatty Acids (FFAs) from tilapia oil

The Free Fatty Acids (FFAs) of tilapia oil were obtained according to [93] with some modifications. In short, 100 g of purified oil and ethanolic KOH solution (3:1, alcohol/oil) were heated to 75 °C and reacted for 2 h under mechanical stirring at 400 rpm. The mass of KOH (40.6 g) used in the preparation of the ethanolic solution was determined from the saponification index value of the oil, with an increase of 10% to guarantee the complete reaction. At the end of the reaction, the mixture was transferred to a separatory funnel and washed with 6M HCl solution to pH 2.0. The upper oil phase, containing 200 mL of ethyl acetate, was washed with distilled water to neutral pH. The solvent was removed by rotary evaporator [93].

3.2.15. Production of Biolubricant Ester

The production of the biolubricant ester was conducted in Eppendorf tubes (2 mL) in orbital shaker incubators at 200 rpm. The esterification was conducted using the FFAs obtained from the hydrolysis of the tilapia oil and 2-ethyl-1-hexanol as substrates, with molar ratio (acid:alcohol) 1:1. The reaction was started by adding 2% (mass of oil) CALA-MNP (and incubated at 3 for 24 h. After the specific reaction time for each assay, the acid index of the enzyme-free supernatant was determined for each sample. For this purpose, aliquots of 0.2 g were withdrawn from the reaction volume, diluted in 20 mL of ethyl alcohol and 3 drops phenolphthalein and then titrated with sodium hydroxide (40 mM) (Cavalcanti et al., 2018) [5], with some modifications. The acid index (AI) was established according to Equation (1) [5].

$$AI (mgNaOH/g) = MM_{NaOH} \times Shch_{NaOH} \times f \times \left(\frac{V_{NaOH}}{m} \right) \quad (1)$$

where MM_{NaOH} (g/mol) is the molar mass of NaOH; III_{NaOH} (mol/L) is the molarity of the NaOH solution; f is the correction factor determined by NaOH standardization; V_{NaOH} (mL) is the volume of NaOH spent on the titration; and, m (g) is the mass of the sample to be analyzed. The conversion of FFAs to esters was calculated by Equation (2), considering the acidity at time zero (AI_0) and time t (AI_t) [5].

$$Conversion\ FFA(\%) = \frac{AI_0 - AI_t}{AI_0} \times 100 \quad (2)$$

3.2.16. Operational Stability

Operational stability was checked by consecutive reactions towards the production of the biolubricant ester using 2% for enzyme content, 1:1 for molar ratio (acid:alcohol), 30 °C for temperature and 24 h of reaction time stirred at 200 rpm. Prior to each cycle, the enzyme was separated from the reaction medium by magnetization and washed three times with hexane to remove unreacted substrates [48].

4. Conclusions

Lipase A from *Candida antarctica* was immobilized on chitosan-coated magnetic nanoparticles of iron activated with glutaraldehyde. From immobilization parameters (84.1% ± 1.0 for immobilization yield and 208.0 ± 3.0 U/g ± 1.1 for derivative activity) to thermal and pH inactivation analysis (CALA-MPN half-life was more than 9 times bigger than that for CALA), the great performance of the immobilization procedure was established and confirmed by FTIR, XRPD, TG and SEM analysis.

Author Contributions: Conceptualization, J.C.S. and R.R.C.M.; methodology, R.R.C.M., P.J.M.L., B.B.P., T.M.F. and J.C.S.d.S.; software, R.R.C.M.; validation, R.R.C.M.; formal analysis, R.R.C.M., T.M.F. and L.M.U.D.; investigation, R.R.C.M., P.J.M.L., B.B.P., T.M.F.; resources, J.C.S., M.C.M.d.S., R.F.-L., P.B.A.F. and L.R.B.G.; data curation, P.B.A.F. and L.R.B.G.; writing—original draft preparation, R.R.C.M.; writing—review and editing, J.C.S.d.S., R.F.-L., M.C.M.d.S., P.B.A.F. and L.R.B.G.; visualization, J.C.S. and R.F.-L.; supervision, J.C.S. and M.C.M.d.S.; project administration, J.C.S. and M.C.M.d.S.; funding acquisition, J.C.S.d.S., M.C.M.d.S. and P.B.A.F.

Funding: This research was funded by Fundação Cearense de Apoio ao Desenvolvimento Científico e Tecnológico (FUNCAP), grant numbers BP3-0139-00005.01.00/18 and PNE-0112-00048.01.00/16, Conselho Nacional de Desenvolvimento Científico e Tecnológico (CNPq), grant numbers 422942/2016-2, 409058/2015-5 and 408790/2016-4, Coordenação de Aperfeiçoamento de Ensino Superior (CAPES-Finance Code 001) and MICIU, grant number CTQ2015-68951-C3-3-R.

Acknowledgments: The authors would like to thank the Brazilian research-funding agencies Fundação Cearense de Apoio ao Desenvolvimento Científico e Tecnológico (FUNCAP), Conselho Nacional de Desenvolvimento Científico e Tecnológico (CNPq), Coordenação de Aperfeiçoamento de Ensino Superior (CAPES) and Ministerio de Economía y Competitividad and FEDER funds. In addition, the authors also acknowledge Central Analítica-UFC/CT-INFRA/MCTI-SISNANO/Pró-Equipamentos. The authors would like to thank Maria Alexandra de Sousa Rios, Departamento de Engenharia Mecânica-UFC, for providing tilapia fish viscera oil for this study.

Conflicts of Interest: The authors declare no conflict of interest.

References

1. Chowdhury, A.; Mitra, D.; Biswas, D. Biolubricant synthesis from waste cooking oil via enzymatic hydrolysis followed by chemical esterification: Biolubricant synthesis from waste cooking oil. *J. Chem. Technol. Biotechnol.* **2013**, *88*, 139–144. [[CrossRef](#)]
2. Linko, Y.-Y.; Lämsä, M.; Huhtala, A.; Linko, P. Lipase-catalyzed transesterification of rapeseed oil and 2-ethyl-1-hexanol. *J. Am. Oil Chem. Soc.* **1994**, *71*, 1411–1414. [[CrossRef](#)]
3. Kleinaite, E.; Jaška, V.; Tvaska, B.; Matijošytė, I. A cleaner approach for biolubricant production using biodiesel as a starting material. *J. Clean. Prod.* **2014**, *75*, 40–44. [[CrossRef](#)]
4. Chowdhury, A.; Chakraborty, R.; Mitra, D.; Biswas, D. Optimization of the production parameters of octyl ester biolubricant using Taguchi's design method and physico-chemical characterization of the product. *Ind. Crops Prod.* **2014**, *52*, 783–789. [[CrossRef](#)]
5. Cavalcanti, E.D.C.; Aguiéiras, É.C.G.; da Silva, P.R.; Duarte, J.G.; Cipolatti, E.P.; Fernandez-Lafuente, R.; da Silva, J.A.C.; Freire, D.M.G. Improved production of biolubricants from soybean oil and different polyols via esterification reaction catalyzed by immobilized lipase from *Candida rugosa*. *Fuel* **2018**, *215*, 705–713. [[CrossRef](#)]
6. Sharma, B.K.; Biresaw, G. *Environmentally Friendly and Biobased Lubricants*; CRC Press: Boca Raton, FL, USA, 2017; p. 434.
7. Fernandes, K.V.; Papadaki, A.; da Silva, J.A.C.; Fernandez-Lafuente, R.; Koutinas, A.A.; Freire, D.M.G. Enzymatic esterification of palm fatty-acid distillate for the production of polyol esters with biolubricant properties. *Ind. Crops Prod.* **2018**, *116*, 90–96. [[CrossRef](#)]
8. Da Silva, J.A.C.; Soares, V.F.; Fernandez-Lafuente, R.; Habert, A.C.; Freire, D.M.G. Enzymatic production and characterization of potential biolubricants from castor bean biodiesel. *J. Mol. Catal. B Enzym.* **2015**, *122*, 323–329. [[CrossRef](#)]
9. Greco-Duarte, J.; Cavalcanti-Oliveira, E.D.; Da Silva, J.A.C.; Fernandez-Lafuente, R.; Freire, D.M.G. Two-step enzymatic production of environmentally friendly biolubricants using castor oil: Enzyme selection and product characterization. *Fuel* **2017**, *202*, 196–205. [[CrossRef](#)]
10. De Oliveira, U.M.F.; de Lima Matos, L.J.B.; de Souza, M.C.M.; Pinheiro, B.B.; dos Santos, J.C.S.; Gonçalves, L.R.B. Effect of the presence of surfactants and immobilization conditions on catalysts' properties of *Rhizomucor miehei* Lipase onto Chitosan. *Appl. Biochem. Biotechnol.* **2018**, *184*, 1263–1285. [[CrossRef](#)]
11. Zhang, Y.; Dai, Y.; Hou, M.; Li, T.; Ge, J.; Liu, Z. Chemo-enzymatic synthesis of valrubicin using Pluronic conjugated lipase with temperature responsiveness in organic media. *RSC Adv.* **2013**, *3*, 22963. [[CrossRef](#)]
12. Gharat, N.; Rathod, V.K. Enzyme catalyzed transesterification of waste cooking oil with dimethyl carbonate. *J. Mol. Catal. B Enzym.* **2013**, *88*, 36–40. [[CrossRef](#)]
13. Villalba, M.; Verdasco-Martín, C.M.; dos Santos, J.C.S.; Fernandez-Lafuente, R.; Otero, C. Operational stabilities of different chemical derivatives of Novozym 435 in an alcoholysis reaction. *Enzyme Microb. Technol.* **2016**, *90*, 35–44. [[CrossRef](#)]
14. Palla, C.A.; Pacheco, C.; Carrín, M.E. Production of structured lipids by acidolysis with immobilized *Rhizomucor miehei* lipases: Selection of suitable reaction conditions. *J. Mol. Catal. B Enzym.* **2012**, *76*, 106–115. [[CrossRef](#)]
15. Törnvall, U.; Orellana-Coca, C.; Hatti-Kaul, R.; Adlercreutz, D. Stability of immobilized *Candida antarctica* lipase B during chemo-enzymatic epoxidation of fatty acids. *Enzyme Microb. Technol.* **2007**, *40*, 447–451. [[CrossRef](#)]
16. Akanbi, T.O.; Barrow, C.J. *Candida antarctica* lipase A effectively concentrates DHA from fish and thraustochytrid oils. *Food Chem.* **2017**, *229*, 509–516. [[CrossRef](#)]
17. Kasche, V.; Haufler, U.; Riechmann, L. Equilibrium and kinetically controlled synthesis with enzymes: Semisynthesis of penicillins and peptides. In *Methods in Enzymology*; Elsevier: Amsterdam, The Netherlands, 1987; pp. 280–292.
18. Bolsoni-Lopes, A.; Alonso-Vale, M.I.C. Lipolysis and lipases in white adipose tissue—An update. *Arch. Endocrinol. Metab.* **2015**, *59*, 335–342. [[CrossRef](#)]
19. Robles-Medina, A.; González-Moreno, P.A.; Esteban-Cerdán, L.; Molina-Grima, E. Biocatalysis: Towards ever greener biodiesel production. *Biotechnol. Adv.* **2009**, *27*, 398–408. [[CrossRef](#)]

20. Uppenberg, J.; Patkar, S.; Bergfors, T.; Jones, T.A. Crystallization and preliminary X-ray studies of lipase B from *Candida antarctica*. *J. Mol. Biol.* **1994**, *235*, 790–792. [[CrossRef](#)]
21. Ericsson, D.J.; Kasrayan, A.; Johansson, P.; Bergfors, T.; Sandström, A.G.; Bäckvall, J.-E.; Mowbray, S.L. X-ray Structure of *Candida antarctica* lipase A shows a novel lid structure and a likely mode of interfacial activation. *J. Mol. Biol.* **2008**, *376*, 109–119. [[CrossRef](#)]
22. Zamost, B.L.; Nielsen, H.K.; Starnes, R.L. Thermostable enzymes for industrial applications. *J. Ind. Microbiol.* **1991**, *8*, 71–81. [[CrossRef](#)]
23. Arana-Peña, S.; Lokha, Y.; Fernández-Lafuente, R. Immobilization on octyl-agarose beads and some catalytic features of commercial preparations of lipase a from *Candida antarctica* (Novocor ADL): Comparison with immobilized lipase B from *Candida antarctica*. *Biotechnol. Prog.* **2019**, *35*, e2735. [[CrossRef](#)]
24. Datta, S.; Christena, L.R.; Rajaram, Y.R.S. Enzyme immobilization: An overview on techniques and support materials. *3 Biotech* **2013**, *3*, 1–9. [[CrossRef](#)]
25. Dos Santos, J.C.S.; Bonazza, H.L.; de Matos, L.J.B.L.; Carneiro, E.A.; Barbosa, O.; Fernandez-Lafuente, R.; Gonçalves, L.R.B.; de Sant' Ana, H.B.; Santiago-Aguiar, R.S. Immobilization of CALB on activated chitosan: Application to enzymatic synthesis in supercritical and near-critical carbon dioxide. *Biotechnol. Rep.* **2017**, *14*, 16–26. [[CrossRef](#)]
26. Barbosa, O.; Torres, R.; Ortiz, C.; Berenguer-Murcia, Á.; Rodrigues, R.C.; Fernandez-Lafuente, R. Heterofunctional supports in enzyme immobilization: From traditional immobilization protocols to opportunities in tuning enzyme properties. *Biomacromolecules* **2013**, *14*, 2433–2462. [[CrossRef](#)]
27. Mateo, C.; Palomo, J.M.; Fernandez-Lorente, G.; Guisan, J.M.; Fernandez-Lafuente, R. Improvement of enzyme activity, stability and selectivity via immobilization techniques. *Enzyme Microb. Technol.* **2007**, *40*, 1451–1463. [[CrossRef](#)]
28. Hanefeld, U.; Gardossi, L.; Magner, E. Understanding enzyme immobilisation. *Chem. Soc. Rev.* **2009**, *38*, 453–468. [[CrossRef](#)]
29. Sheldon, R.A.; van Pelt, S. Enzyme immobilisation in biocatalysis: Why, what and how. *Chem. Soc. Rev.* **2013**, *42*, 6223–6235. [[CrossRef](#)]
30. Garcia-Galan, C.; Berenguer-Murcia, Á.; Fernandez-Lafuente, R.; Rodrigues, R.C. Potential of different enzyme immobilization strategies to improve enzyme performance. *Adv. Synth. Catal.* **2011**, *353*, 2885–2904. [[CrossRef](#)]
31. Rodrigues, R.C.; Ortiz, C.; Berenguer-Murcia, Á.; Torres, R.; Fernández-Lafuente, R. Modifying enzyme activity and selectivity by immobilization. *Chem. Soc. Rev.* **2013**, *42*, 6290–6307. [[CrossRef](#)]
32. Zainal, N.A.; Zulkifli, N.W.M.; Gulzar, M.; Masjuki, H.H. A review on the chemistry, production, and technological potential of bio-based lubricants. *Renew. Sustain. Energy Rev.* **2018**, *82*, 80–102. [[CrossRef](#)]
33. Shahabuddin, M.; Masjuki, H.H.; Kalam, M.A.; Bhuiya, M.M.K.; Mehat, H. Comparative tribological investigation of bio-lubricant formulated from a non-edible oil source (*Jatropha oil*). *Ind. Crops Prod.* **2013**, *47*, 323–330. [[CrossRef](#)]
34. Singh, Y.; Farooq, A.; Raza, A.; Mahmood, M.A.; Jain, S. Sustainability of a non-edible vegetable oil based bio-lubricant for automotive applications: A review. *Process Saf. Environ. Prot.* **2017**, *111*, 701–713. [[CrossRef](#)]
35. Munoz, R.A.; Fernandes, D.M.; Santos, D.Q.; Barbosa, T.G.; Sousa, R.M. Biodiesel: Production, characterization, metallic corrosion and analytical methods for contaminants. In *Biodiesel—Feedstocks, Production and Applications*; InTech Open: London, UK, 2012; pp. 129–175.
36. Nagendramma, P.; Kaul, S. Development of ecofriendly/biodegradable lubricants: An overview. *Renew. Sustain. Energy Rev.* **2012**, *16*, 764–774. [[CrossRef](#)]
37. Kumar, A.; Sharma, S. Potential non-edible oil resources as biodiesel feedstock: An Indian perspective. *Renew. Sustain. Energy Rev.* **2011**, *15*, 1791–1800. [[CrossRef](#)]
38. Singh, D.; Singh, S.P. Low cost production of ester from non edible oil of *Argemone mexicana*. *Biomass Bioenergy* **2010**, *34*, 545–549. [[CrossRef](#)]
39. Le Clef, E.; Kemper, T. Sunflower seed preparation and oil extraction. In *Sunflower*; Elsevier: Amsterdam, The Netherlands, 2015; pp. 187–226.
40. Hamid, H.A.; Yunus, R.; Rashid, U.; Choong, T.S.Y.; Al-Muhtaseb, A.H. Synthesis of palm oil-based trimethylolpropane ester as potential biolubricant: Chemical kinetics modeling. *Chem. Eng. J.* **2012**, *200–202*, 532–540. [[CrossRef](#)]

41. Jayadas, N.H.; Nair, K.P.; Ajithkumar, G. Tribological evaluation of coconut oil as an environment-friendly lubricant. *Tribol. Int.* **2007**, *40*, 350–354. [[CrossRef](#)]
42. Ting, C.-C.; Chen, C.-C. Viscosity and working efficiency analysis of soybean oil based bio-lubricants. *Measurement* **2011**, *44*, 1337–1341. [[CrossRef](#)]
43. Do Valle, C.P.; Rodrigues, J.S.; Fachine, L.M.U.D.; Cunha, A.P.; Queiroz Malveira, J.; Luna, F.M.T.; Ricardo, N.M.P.S. Chemical modification of Tilapia oil for biolubricant applications. *J. Clean. Prod.* **2018**, *191*, 158–166. [[CrossRef](#)]
44. Martins, G.I.; Secco, D.; Tokura, L.K.; Bariccatti, R.A.; Dolci, B.D.; Santos, R.F. Potential of tilapia oil and waste in biodiesel production. *Renew. Sustain. Energy Rev.* **2015**, *42*, 234–239. [[CrossRef](#)]
45. Roriz, G.D.; Delphino, M.K.D.V.C.; Gardner, I.A.; Gonçalves, V.S.P. Characterization of tilapia farming in net cages at a tropical reservoir in Brazil. *Aquac. Rep.* **2017**, *6*, 43–48. [[CrossRef](#)]
46. Silva, J.F.X.; Ribeiro, K.; Silva, J.F.; Cahú, T.B.; Bezerra, R.S. Utilization of tilapia processing waste for the production of fish protein hydrolysate. *Animal Feed Sci. Technol.* **2014**, *196*, 96–106. [[CrossRef](#)]
47. Villamil, O.; Váquiro, H.; Solanilla, J.F. Fish viscera protein hydrolysates: Production, potential applications and functional and bioactive properties. *Food Chem.* **2017**, *224*, 160–171. [[CrossRef](#)]
48. De Souza, M.C.M.; dos Santos, K.P.; Freire, R.M.; Barreto, A.C.H.; Fachine, P.B.A.; Gonçalves, L.R.B. Production of flavor esters catalyzed by lipase B from *Candida antarctica* immobilized on magnetic nanoparticles. *Braz. J. Chem. Eng.* **2017**, *34*, 681–690. [[CrossRef](#)]
49. Netto, C.G.C.M.; Toma, H.E.; Andrade, L.H. Superparamagnetic nanoparticles as versatile carriers and supporting materials for enzymes. *J. Mol. Catal. B Enzym.* **2013**, *85–86*, 71–92. [[CrossRef](#)]
50. Zhou, G.; Fung, K.K.; Wong, L.W.; Chen, Y.; Renneberg, R.; Yang, S. Immobilization of glucose oxidase on rod-like and vesicle-like mesoporous silica for enhancing current responses of glucose biosensors. *Talanta* **2011**, *84*, 659–665. [[CrossRef](#)]
51. Li, X.; Zhu, H.; Feng, J.; Zhang, J.; Deng, X.; Zhou, B.; Zhang, H.; Xue, D.; Li, F.; Mellors, N.J.; et al. One-pot polyol synthesis of graphene decorated with size- and density-tunable Fe₃O₄ nanoparticles for porcine pancreatic lipase immobilization. *Carbon* **2013**, *60*, 488–497. [[CrossRef](#)]
52. Cipolatti, E.P.; Valério, A.; Henriques, R.O.; Moritz, D.E.; Ninow, J.L.; Freire, D.M.G.; Manoel, E.A.; Fernandez-Lafuente, R.; de Oliveira, D. Nanomaterials for biocatalyst immobilization—State of the art and future trends. *RSC Adv.* **2016**, *6*, 104675–104692. [[CrossRef](#)]
53. Xu, W.; Ling, P.; Zhang, T. Polymeric micelles, a promising drug delivery system to enhance bioavailability of poorly water-soluble drugs. *J. Drug Deliv.* **2013**, *2013*, 340315. [[CrossRef](#)]
54. Bilal, M.; Zhao, Y.; Rasheed, T.; Iqbal, H.M.N. Magnetic nanoparticles as versatile carriers for enzymes immobilization: A review. *Int. J. Biol. Macromol.* **2018**, *120*, 2530–2544. [[CrossRef](#)]
55. Sinha, V.R.; Singla, A.K.; Wadhawan, S.; Kaushik, R.; Kumria, R.; Bansal, K.; Dhawan, S. Chitosan microspheres as a potential carrier for drugs. *Int. J. Pharm.* **2004**, *274*, 1–33. [[CrossRef](#)]
56. Silva, J.A.; Macedo, G.P.; Rodrigues, D.S.; Giordano, R.L.C.; Gonçalves, L.R.B. Immobilization of *Candida antarctica* lipase B by covalent attachment on chitosan-based hydrogels using different support activation strategies. *Biochem. Eng. J.* **2012**, *60*, 16–24. [[CrossRef](#)]
57. Anitha, A.; Sowmya, S.; Kumar, P.T.S.; Deepthi, S.; Chennazhi, K.P.; Ehrlich, H.; Tsurkan, M.; Jayakumar, R. Chitin and chitosan in selected biomedical applications. *Prog. Polym. Sci.* **2014**, *39*, 1644–1667. [[CrossRef](#)]
58. Khwaldia, K.; Basta, A.H.; Aloui, H.; El-Saied, H. Chitosan-caseinate bilayer coatings for paper packaging materials. *Carbohydr. Polym.* **2014**, *99*, 508–516. [[CrossRef](#)]
59. Badawi, M.A.; Negm, N.A.; Abou Kana, M.T.H.; Hefni, H.H.; Abdel Moneem, M.M. Adsorption of aluminum and lead from wastewater by chitosan-tannic acid modified biopolymers: Isotherms, kinetics, thermodynamics and process mechanism. *Int. J. Biol. Macromol.* **2017**, *99*, 465–476. [[CrossRef](#)]
60. Oliveira, H.C.; Gomes, B.C.R.; Pelegrino, M.T.; Seabra, A.B. Nitric oxide-releasing chitosan nanoparticles alleviate the effects of salt stress in maize plants. *Nitric Oxide* **2016**, *61*, 10–19. [[CrossRef](#)]
61. Krajewska, B. Application of chitin- and chitosan-based materials for enzyme immobilizations: A review. *Enzyme Microb. Technol.* **2004**, *35*, 126–139. [[CrossRef](#)]
62. Pinheiro, B.B.; Rios, N.S.; Rodríguez Aguado, E.; Fernandez-Lafuente, R.; Freire, T.M.; Fachine, P.B.A.; dos Santos, J.C.S.; Gonçalves, L.R.B. Chitosan activated with divinyl sulfone: A new heterofunctional support for enzyme immobilization. Application in the immobilization of lipase B from *Candida antarctica*. *Int. J. Biol. Macromol.* **2019**, *130*, 798–809. [[CrossRef](#)]

63. Nicolás, P.; Saleta, M.; Troiani, H.; Zysler, R.; Lassalle, V.; Ferreira, M.L. Preparation of iron oxide nanoparticles stabilized with biomolecules: Experimental and mechanistic issues. *Acta Biomater.* **2013**, *9*, 4754–4762. [[CrossRef](#)]
64. Freire, T.M.; Dutra, L.M.U.; Queiroz, D.C.; Ricardo, N.M.P.S.; Barreto, K.; Denardin, J.C.; Wurm, F.R.; Sousa, C.P.; Correia, A.N.; de Lima-Neto, P.; et al. Fast ultrasound assisted synthesis of chitosan-based magnetite nanocomposites as a modified electrode sensor. *Carbohydr. Polym.* **2016**, *151*, 760–769. [[CrossRef](#)]
65. Shete, P.B.; Patil, R.M.; Thorat, N.D.; Prasad, A.; Ningthoujam, R.S.; Ghosh, S.J.; Pawar, S.H. Magnetic chitosan nanocomposite for hyperthermia therapy application: Preparation, characterization and in vitro experiments. *Appl. Surf. Sci.* **2014**, *288*, 149–157. [[CrossRef](#)]
66. De Andrades, D.; Graebin, N.G.; Kadowaki, M.K.; Ayub, M.A.Z.; Fernandez-Lafuente, R.; Rodrigues, R.C. Immobilization and stabilization of different β -glucosidases using the glutaraldehyde chemistry: Optimal protocol depends on the enzyme. *Int. J. Biol. Macromol.* **2019**, *129*, 672–678. [[CrossRef](#)]
67. Vazquez-Ortega, P.G.; Alcaraz-Fructuoso, M.T.; Rojas-Contreras, J.A.; López-Miranda, J.; Fernandez-Lafuente, R. Stabilization of dimeric β -glucosidase from *Aspergillus niger* via glutaraldehyde immobilization under different conditions. *Enzyme Microb. Technol.* **2018**, *110*, 38–45. [[CrossRef](#)]
68. Dos Santos, J.C.S.; Rueda, N.; Barbosa, O.; Fernández-Sánchez, J.F.; Medina-Castillo, A.L.; Ramón-Márquez, T.; Arias-Martos, M.C.; Millán-Linares, M.C.; Pedroche, J.; del Yust, M.M.; et al. Characterization of supports activated with divinyl sulfone as a tool to immobilize and stabilize enzymes via multipoint covalent attachment. Application to chymotrypsin. *RSC Adv.* **2015**, *5*, 20639–20649. [[CrossRef](#)]
69. Barbosa, O.; Ortiz, C.; Berenguer-Murcia, Á.; Torres, R.; Rodrigues, R.C.; Fernandez-Lafuente, R. Glutaraldehyde in bio-catalysts design: A useful crosslinker and a versatile tool in enzyme immobilization. *RSC Adv.* **2014**, *4*, 1583–1600. [[CrossRef](#)]
70. Ait Braham, S.; Hussain, F.; Morellon-Sterling, R.; Kamal, S.; Kornecki, J.F.; Barbosa, O.; Kati, D.E.; Fernandez-Lafuente, R. Cooperativity of covalent attachment and ion exchange on alcalase immobilization using glutaraldehyde chemistry: Enzyme stabilization and improved proteolytic activity. *Biotechnol. Prog.* **2019**, *35*, e2768. [[CrossRef](#)]
71. Zaak, H.; Peirce, S.; de Albuquerque, T.; Sassi, M.; Fernandez-Lafuente, R. Exploiting the versatility of aminated supports activated with glutaraldehyde to immobilize β -galactosidase from *Aspergillus oryzae*. *Catalysts* **2017**, *7*, 250. [[CrossRef](#)]
72. Osuna, Y.; Sandoval, J.; Saade, H.; López, R.G.; Martínez, J.L.; Colunga, E.M.; de la Cruz, G.; Segura, E.P.; Arévalo, F.J.; Zon, M.A.; et al. Immobilization of *Aspergillus niger* lipase on chitosan-coated magnetic nanoparticles using two covalent-binding methods. *Bioprocess Biosyst. Eng.* **2015**, *38*, 1437–1445. [[CrossRef](#)]
73. Rodrigues, D.S.; Mendes, A.A.; Adriano, W.S.; Gonçalves, L.R.B.; Giordano, R.L. Multipoint covalent immobilization of microbial lipase on chitosan and agarose activated by different methods. *J. Mol. Catal. B Enzym.* **2008**, *51*, 100–109. [[CrossRef](#)]
74. Berger, J.; Reist, M.; Mayer, J.M.; Felt, O.; Peppas, N.A.; Gurny, R. Structure and interactions in covalently and ionically crosslinked chitosan hydrogels for biomedical applications. *Eur. J. Pharm. Biopharm.* **2004**, *57*, 19–34. [[CrossRef](#)]
75. Kirk, O.; Christensen, M.W. Lipases from *Candida antarctica*: Unique Biocatalysts from a Unique Origin. *Org. Process Res. Dev.* **2002**, *6*, 446–451. [[CrossRef](#)]
76. Heldt-Hansen, H.P.; Ishii, M.; Patkar, S.A.; Hansen, T.T.; Eigtved, P. A new immobilized positional nonspecific lipase for fat modification and ester synthesis. In *Biocatalysis in Agricultural Biotechnology*; Whitaker, J.R., Sonnet, P.E., Eds.; American Chemical Society: Washington, DC, USA, 1989; Volume 389, pp. 158–172. ISBN 978-0-8412-1571-9.
77. Zaak, H.; Fernandez-Lopez, L.; Velasco-Lozano, S.; Alcaraz-Fructuoso, M.T.; Sassi, M.; Lopez-Gallego, F.; Fernandez-Lafuente, R. Effect of high salt concentrations on the stability of immobilized lipases: Dramatic deleterious effects of phosphate anions. *Process Biochem.* **2017**, *62*, 128–134. [[CrossRef](#)]
78. Martinelle, M.; Holmquist, M.; Hult, K. On the interfacial activation of *Candida antarctica* lipase A and B as compared with *Humicola lanuginosa* lipase. *Biochim. Biophys. Acta Lipids Lipid Metab.* **1995**, *1258*, 272–276. [[CrossRef](#)]
79. Melo, A.; Silva, F.; dos Santos, J.; Fernández-Lafuente, R.; Lemos, T.; Dias Filho, F. Synthesis of benzyl acetate catalyzed by lipase immobilized in nontoxic chitosan-polyphosphate beads. *Molecules* **2017**, *22*, 2165. [[CrossRef](#)]

80. Yang, X.; Liu, L.; Zhang, M.; Tan, W.; Qiu, G.; Zheng, L. Improved removal capacity of magnetite for Cr(VI) by electrochemical reduction. *J. Hazard. Mater.* **2019**, *374*, 26–34. [[CrossRef](#)]
81. Long, J.; Yu, X.; Xu, E.; Wu, Z.; Xu, X.; Jin, Z.; Jiao, A. In situ synthesis of new magnetite chitosan/carrageenan nanocomposites by electrostatic interactions for protein delivery applications. *Carbohydr. Polym.* **2015**, *131*, 98–107. [[CrossRef](#)]
82. El-Guendouz, S.; Aazza, S.; Lyoussi, B.; Bankova, V.; Lourenço, J.; Costa, A.; Mariano, J.; Miguel, M.; Faleiro, M. Impact of biohybrid magnetite nanoparticles and moroccan propolis on adherence of methicillin resistant strains of staphylococcus aureus. *Molecules* **2016**, *21*, 1208. [[CrossRef](#)]
83. Rasoulzadeh, H.; Mohseni-Bandpei, A.; Hosseini, M.; Safari, M. Mechanistic investigation of ciprofloxacin recovery by magnetite-imprinted chitosan nanocomposite: Isotherm, kinetic, thermodynamic and reusability studies. *Int. J. Biol. Macromol.* **2019**, *133*, 712–721. [[CrossRef](#)]
84. Neto, C.G.T.; Giacometti, J.A.; Job, A.E.; Ferreira, F.C.; Fonseca, J.L.C.; Pereira, M.R. Thermal analysis of chitosan based networks. *Carbohydr. Polym.* **2005**, *62*, 97–103. [[CrossRef](#)]
85. Ziegler-Borowska, M.; Chełminiak, D.; Kaczmarek, H. Thermal stability of magnetic nanoparticles coated by blends of modified chitosan and poly(quaternary ammonium) salt. *J. Therm. Anal. Calorim.* **2015**, *119*, 499–506. [[CrossRef](#)]
86. Poon, L.; Wilson, L.D.; Headley, J.V. Chitosan-glutaraldehyde copolymers and their sorption properties. *Carbohydr. Polym.* **2014**, *109*, 92–101. [[CrossRef](#)] [[PubMed](#)]
87. Silva, N.C.A.; Miranda, J.S.; Bolina, I.C.A.; Silva, W.C.; Hirata, D.B.; de Castro, H.F.; Mendes, A.A. Immobilization of porcine pancreatic lipase on poly-hydroxybutyrate particles for the production of ethyl esters from macaw palm oils and pineapple flavor. *Biochem. Eng. J.* **2014**, *82*, 139–149. [[CrossRef](#)]
88. Reis, C.; Sousa, E.; Serpa, J.; Oliveira, R.; Oliveira, R.; Santos, J. Design of immobilized enzyme biocatalysts: Drawbacks and opportunities. *Quim. Nova* **2019**, *42*, 768–783. [[CrossRef](#)]
89. Xie, W.; Ma, N. Immobilized lipase on Fe₃O₄ nanoparticles as biocatalyst for biodiesel production. *Energy Fuels* **2009**, *23*, 1347–1353. [[CrossRef](#)]
90. Bezerra, R.M.; Neto, D.M.A.; Galvão, W.S.; Rios, N.S.; Carvalho, A.C.L.D.M.; Correa, M.A.; Bohn, F.; Fernandez-Lafuente, R.; Fechine, P.B.A.; de Mattos, M.C.; et al. Design of a lipase-nano particle biocatalysts and its use in the kinetic resolution of medicament precursors. *Biochem. Eng. J.* **2017**, *125*, 104–115. [[CrossRef](#)]
91. De Souza, T.C.; Fonseca, T.D.S.; da Costa, J.A.; Rocha, M.V.P.; de Mattos, M.C.; Fernandez-Lafuente, R.; Gonçalves, L.R.B.; dos Santos, J.C. Cashew apple bagasse as a support for the immobilization of lipase B from *Candida antarctica*: Application to the chemoenzymatic production of (R)-Indanol. *J. Mol. Catal. B Enzym.* **2016**, *130*, 58–69. [[CrossRef](#)]
92. Bradford, M.M. A rapid and sensitive method for the quantitation of microgram quantities of protein utilizing the principle of protein-dye binding. *Anal. Biochem.* **1976**, *72*, 248–254. [[CrossRef](#)]
93. Ishak, A.A.; Salimon, J. Synthesis of rubber seed oil and trimethylolpropane based biolubricant base stocks. *Malays. J. Anal. Sci.* **2013**, *17*, 414–421.

